Effects of *Tremella fuciformis*-Derived Polysaccharides with Different Molecular Weight on D-Galactose-Induced Aging of Mice

Donghui Luo[1] , Xiaofei Liu[1] , Jingjing Guan[1] , Guili Jiang[1] , Yanglin Hua[1] , Xinfei Zhang[2] , Xiaofei Xu[1]*

[1]College of Food Science and Engineering, Guangdong Ocean University, Yangjiang 529500, PR China
[2]College of Food Science and Engineering, South China University of Technology, Guangzhou 510640, PR China

The structure-bioactivity relationship of *Tremella fuciformis* polysaccharides (TFPs) in anti-aging *in vivo* is rarely reported. In the present study, a purified TFP, named HM, mainly composed of mannose, fucose, xylose, and glucose in a molar ratio of 4.14:0.98:0.81:0.62, was obtained from the fruiting body of *T. fuciformis*. Subsequently, two differentially degraded TFPs, named MM and LM, respectively, were prepared by a combined method of ultrasonic irradiation (US) and H_2O_2 treatment. Their structural properties, scavenging activities against free radicals *in vitro*, and anti-aging effects on D-galactose-induced aging of mice were determined. The average molecular weight of HM, MM, and LM was 58.3×10^6, 4.68×10^6, and 3.14×10^5 Da, respectively. All three TFPs were devoid of triple helix conformation and exhibited concentration- and molecular weight--dependent scavenging activity against radicals. The TFPs markedly relieved skin aging, effectively attenuated oxidative stress, and significantly decreased inflammation in D-galactose-induced aging mice. MM exhibited the best anti-aging effect among the TFPs. Additionally, TFPs partially restored the alterations in pH and the total content of short-chain fatty acids (SCFAs) in the colon but exhibited various impacts on the content of the individual SCFAs. These findings would provide rational guidance for a better application of TFPs in anti-aging foods and expand our understanding of the structure-function relationship of mushroom polysaccharides.

Key words: mushroom, polysaccharide purification, anti-oxidant activity, anti-aging activity, structure-function relationship, anti-oxidant enzyme

INTRODUCTION

Mushrooms have been a part of human diet for centuries and have been proven to confer a number of benefits against human diseases, such as cancer, infection, atherosclerosis, diabetes, neurodegenerative conditions, *etc.*, in addition to their nutritional and culinary values [Venturella *et al.*, 2021]. Polysaccharides in mushrooms are considered the main active components responsible for their health-promoting benefits [Huang & Nie, 2015]. Numerous studies have documented the structural properties of polysaccharides, such as monosaccharide composition, molecular weight, and conformation, to be closely associated with their bioactivities [Ferreira *et al.*, 2015]. For example, the anti-tumor activity of β-glucan derived from *Lentinula edodes* strongly depends on its triple-helical conformation [Zhang *et al.*, 2005]. Degraded polysaccharides from *Ganoderma lucidum* with a lower molecular weight (13.6 kDa) have higher hypolipidemic and antioxidant activities in high-fat diet-induced obese mice than the original polysaccharides (3,060 kDa) [Xu *et al.*, 2019]. Thus, exploring the structure-bioactivity relationship of mushroom polysaccharides contributes to a better development and application of polysaccharides for the prevention and/or management of human diseases.

Tremella fuciformis, commonly named snow ear, has been consumed as food and used in traditional Chinese medicine for hundreds of years for its nutritional and health beneficial value [Wu *et al.*, 2019]. *T. fuciformis* polysaccharides (TFPs) exhibit a variety of bioactivities, including anti-tumor and immune modulation, anti-oxidation and anti-aging, hypoglycemic and hypocholesterolemic effects, neuroprotection, *etc*. [Wu *et al.*, 2019; Yang *et al.*, 2019]. TFPs not only reduce the levels of free radicals *in vitro* [Ge *et al.*, 2020; Li *et al.*, 2020], but also show protective effects of antioxidant enzymes in aging animal models *in vivo* [Zhang *et al.*, 2014], indicating their great potential in the management of oxidative stress-induced health problems. To date, many different structures of TFPs have been reported, which vary greatly depending on the sources, extraction methods, and purification processes [Wu *et al.*, 2019]. For instance, the molecular weight of TFPs reported in different studies ranges from 1.08×10^3 to 3.74×10^6 Da [Wu *et al.*, 2019; Yang *et al.*, 2019]. Previous research indicated that TFPs with a low molecular weight showed high anti-oxidant activity *in vitro* [Li *et al.*, 2020]. However, the *in vitro* model cannot simulate the internal conditions within cells [Heinrich *et al.*, 2020]. Considering the great differences in the biochemical circumstances between *in vitro* assays and within cells in an organism, it is necessary to investigate the relationship between the structure and bioactivity of TFPs from the view of mammalian model to promote a better application of TFPs in functional foods and nutraceuticals.

In the present study, to better focus our attention on the effect of *T. fuciformis* polysaccharides with different molecular weights on anti-aging activities *in vivo*, a high-molecular-weight TFP was first obtained from the fruiting body of *T. fuciformis*. Then, two differentially degraded TFPs were prepared from the above TFP using a combined method of ultrasonic irradiation (US) and H_2O_2 treatments. Subsequently, the structural properties of the three TFPs and their anti-oxidant activities against 1,1-diphenyl-2-picrylhydrazyl (DPPH) radical, hydroxyl radical, and superoxide anion radical *in vitro* were examined. Finally, D-galactose-aged mice were used to assess their anti-aging effects *in vivo* by measuring the content of hydroxyproline and hyaluronic acid in the skin; the activity of glutathione peroxidase (GSH-Px) and superoxide dismutase (SOD); the content of malondialdehyde (MDA) in serum, liver, and heart; the level of interleukin 1β (IL-1β) and tumor necrosis factor α (TNF-α) in serum; and the alteration in pH and production of short-chain fatty acids (SCFAs) in the gastrointestinal tract.

MATERIAL AND METHODS

■ TFPs extraction and purification

Dried *T. fuciformis* fruiting bodies were purchased from a local agricultural market in Gutian, Fujian province, China. They were dried by heat air in an electrically-heated oven under normal pressure. First, the *T. fuciformis* fruiting bodies were crushed and sifted through 40 mesh for use. TFPs were extracted using boiling tap water (1:60, *w/v*) for 6 h. The extract solution was then centrifuged (3,000×*g*, 5 min) and the supernatant was concentrated to a quarter of the original weight under vacuum at 70°C. Subsequently, deproteination was performed by adjusting the solution pH to pH 4.0 with citric acid and kept at 4°C for 4 days to enable the complete precipitation of the proteins by the isoelectric precipitation method [Oliveira *et al.*, 1999]. The supernatant was collected and three equivalent volumes of 95% ethanol were added to precipitate polysaccharides at 4°C overnight. The precipitate was collected by centrifugation (5,000×*g*, 5 min) and re-dissolved in distilled water (0.2 g/100 g). Ultra-filtration of the solution with a 50 nm pore size membrane was performed using an ultrafiltration system LDS-L1 (AITESEN Co., Ltd, Suzhou, China). The retained fluid was collected and dialyzed using a dialysis bag (cut-off of 3,000 Da) against distilled water for 4 days. The dialysis solution was freeze-dried to obtain white TFPs powder. No apparent absorption was observed at 260 and 280 nm by ultraviolet scanning (data not shown), suggesting the absence of protein and nucleic acid in the TFPs.

■ Preparation of differentially degraded TFPs

Degraded TFPs were prepared by a combined method of US and H_2O_2 treatment [Li *et al.*, 2020] with slight modifications. Briefly, the original TFPs was dissolved in distilled water to obtain a 0.2 g/100 g solution. H_2O_2 solution was added to the TFPs solution with a final concentration of 0.5 g/100 g. The degradation processes were then conducted in an ultrasonic processor (KQ-250DE, Kunshan Ultrasonic Instrument Co., Ltd, Kunshan, China) by setting the amplitude of 50% on the controller panel. The degradation degree of TFPs was determined by measuring the viscosity of the TFPs solution with a viscometer (DV2T, Brookfield, Middleboro, MA, USA) at 25±0.5°C. The viscosity of the original TFPs solution was 106.7 mPa×s. The viscosity of the moderately degraded TFPs solution and the highly degraded TFPs solution was 22.4 and 5.7 mPa×s, respectively. The degraded TFPs were obtained by dialysis (cut-off of 1,000 Da) and lyophilization. The original TFPs with high molecular weight, moderately degraded TFPs, and highly degraded TFPs were named HM, MM, and LM, respectively.

■ Structure characterization
■ Carbohydrate content and monosaccharide composition analysis

The carbohydrate content of all samples was detected by phenol sulfuric acid analysis with mannose as a standard [Liu *et al.*, 2019]. The monosaccharide composition of HM was detected according to a previous method [Huang *et al.*, 2011] with slight modifications. In brief, 10 mg HM was dissolved with 4 mL of 2 M trifluoroacetic acid in a glass tube, sealed, and hydrolyzed at 121°C for 4 h. Acetylation was performed with 10 mg hydroxylamine hydrochloride and 0.5 mL pyridine for 30 min at 90°C, and next the mixture was cooled to room temperature. Then, 1 mL of acetic anhydride was added to the solution and reacted at 90°C for 30 min to obtain alditol acetate derivative. The alditol acetate derivative was analyzed using a 6890N Agilent gas chromatograph (Agilent, Santa Clara, CA, USA) with a DB-1701 capillary column (30 m×0.25 mm, Agilent). The chromatography

conditions were as follows: nitrogen flow rate: 1 mL/min; inlet temperature: 250℃; evaporation chamber temperature: 250℃; detector temperature: 300℃; injection volume: 1 μL; split ratio: 20:1. Glucose, fucose, mannose, galactose, arabinose, xylose, glucuronic acid, rhamnose were chosen as standards (Sigma-Aldrich, Saint Louis, MO, USA).

■ Nuclear magnetic resonance (NMR) and Fourier transform infrared spectroscopy (FT-IR) analysis

Thirty mg of HM sample were dissolved in 1.5 mL 99% D_2O and then lyophilized. This process was repeated two times. The lyophilized HM was dissolved with 0.8 mL of D_2O, and transferred to an NMR tube. ^{1}H and ^{13}C NMR spectra were obtained on a Bruker AVANCE III HD 600 NMR spectrometer (Bruker, Billerica, MA, USA). FT-IR spectra of the TFPs samples were measured in the range of 4,000–400 cm^{-1} by KBr-disk method using an FT-IR spectrometer (Nicolet IS50-Nicolet Continuum, Thermo Fisher Scientific, Waltham, MA, USA) [Li et al., 2020]. OMNIC software (Thermo Fisher Scientific) was used for spectroscopy analysis.

■ Molecular weight analysis

The molecular weight distribution was determined by high-performance gel permeation chromatography (HPGPC) analysis [Liu et al., 2019]. In brief, TFPs were dissolved to 2 mg/mL in mobile phase (0.02 M KH_2PO_4 solution, pH 6), then the TFP solutions were filtered through a 0.45 μm membrane filter, followed by injection into an HPGPC system (Ultimate 3000, Thermo Fisher Scientific) equipped with Ultrahydrogel 1000 (7.8×300 mm) and Ultrahydrogel 500 (7.8×300 mm) columns (Thermo Fisher Scientific). The flow rate was 0.8 mL/min. A calibration curve was plotted by measuring a series of dextran standards. Each run was recorded for 35 min. Additionally, the conformational characteristic of TFPs in solution was measured using the Congo red approach reported previously [Lee et al., 2009]. Yeast β-glucan (Tokyo Chemical Industry Co., Ltd, Tokyo, Japan) was chosen as a positive control.

■ **Anti-oxidation activity analysis in vitro**
■ Determination of DPPH radical scavenging activity

DPPH radical (DPPH[•]) scavenging activity of TFPs was determined according to the previous method [Ye et al., 2012] with slight modifications. Briefly, 2.0 mL of the TFP solution (150 and 300 μg/mL, respectively) were mixed with 2.0 mL of DPPH[•] (Sigma-Aldrich) dissolved in ethanol (0.02 mg/mL). Subsequently, the mixture was kept in a lucifugal cabinet at room temperature for 30 min. The absorbance of supernatant was measured at 517 nm using an ultraviolet-visible (UV-Vis) spectrophotometer (752N, Shanghai Jingke Scientific Instrument Co., Ltd, Shanghai, China) after centrifugation at 5,000×g for 10 min. Ascorbic acid (AA) was chosen as a positive control. The absorbance of the mixture was measured in triplicate and the test of DPPH[•] scavenging activity was repeated three times. The DPPH[•] scavenging activity was calculated using Equation (1).

$$\text{DPPH}^{•} \text{ scavenging activity (\%)} = (1 - \frac{A_1 - A_2}{A_0}) \times 100 \qquad (1)$$

where: A_1 is the absorbance of the solution containing TFPs and DPPH[•]; A_2 is the absorbance of the solution containing TFPs and ethanol; and A_0 is the absorbance of the solution containing only deionized water and DPPH[•].

■ Determination of hydroxyl radical scavenging activity

The hydroxyl radical ([•]OH) scavenging activity was measured by the previously reported method [Liu et al., 2009] with slight modification. Briefly, the hydroxyl radical was produced by mixing 0.4 mL of 0.2 M sodium phosphate buffer (pH 7.4), 0.6 mL of 5 mM 1,10-phenanthroline, 0.6 mL of 5 mM $FeSO_4$, and 0.8 mL of H_2O_2 (0.1 g/100 g). After adding 0.6 mL of the TFPs solution (150 and 300 μg/mL, respectively) or deionized water, the mixture was incubated at 37℃ for 60 min. The absorbance was determined at 536 nm using a 752N UV-Vis spectrophotometer (Shanghai Jingke Scientific Instrument Co., Ltd) in triplicate. The [•]OH scavenging activity was calculated according to Equation (2).

$$^{•}\text{OH scavenging activity (\%)} = (\frac{A_{sample} - A_{blank}}{A' - A_{sample}}) \times 100 \qquad (2)$$

where: A' is the absorbance of the deionized water instead of H_2O_2; A_{sample} is the absorbance of TFPs solution, and A_{blank} is the absorbance of the deionized solution instead of TFPs solution. AA was used as a positive control. Test was repeated three times.

■ Determination of superoxide anion radical scavenging activity

The superoxide anion radical ($O_2^{•-}$) scavenging activity was determined following the previously described method [Cao et al., 2007] with some modifications. Briefly, 3.0 mL of the TFPs solution (150 and 300 μg/mL, respectively) or deionized water as a blank were added to 3.0 mL of 0.05 M Tris-HCl buffer (pH 8.2). The mixture was shaken thoroughly and incubated at 25℃ for 20 min. Then, 100 μL of 5 mM pyrogallol (1,2,3-trihydroxybenzene) were added to the mixture and incubated at 25℃ for 5 min. The absorbance was recorded at 325 nm using a 752N UV-Vis spectrophotometer (Shanghai Jingke Scientific Instrument Co., Ltd). Test was repeated three times. AA was chosen as a positive control. The $O_2^{•-}$ scavenging activity was estimated using Equation (3).

$$O_2^{•-} \text{ scavenging activity (\%)} = (1 - \frac{A_{sample}}{A_{blank}}) \times 100 \qquad (3)$$

where: A_{sample} is the absorbance of the TFP solution, and A_{blank} is the absorbance of deionized water.

■ **In vivo experiment**
■ Animal and experiment procedure

Specific-pathogen-free (SPF) grade 4-week-old male Kunming mice (body weight, BW, 18±2 g) were purchased from Guangdong Medical Experimental Animal Center and raised in the Laboratory Animals Center at Guangzhou University of Chinese Medicine, Guangzhou, China. The animals were kept under SPF laboratory conditions: the room temperature was kept at 22±2℃ under 60~80% relative humidity with a 12 h light/dark cycle.

Food and water were freely available to mice. Experimental procedures were consistent with the Health Guide for the Care and Use of Laboratory Animals of National Institutes and the China legislation concerning the use and care of laboratory animals and approved by the Ethical Committee of Guangzhou University of Chinese Medicine. After two weeks of adaption to the SPF environment, a total of 40 male mice were randomly assigned to five groups: Normal group, Model group, HM group, MM group, and LM group. Mice in the Normal group were intraperitoneally injected daily with physiological saline, while those in other groups were injected with D-galactose (Macklin Biochemical Co., Shanghai, China) at a dosage of 120 mg/kg of body weight (BW) instead [Zhao *et al.*, 2019]. Mice in the HM, MM, and LM groups were additionally administered orally with HM, MM, and LM, respectively, at a dosage of 100 mg/kg of BW per day. The treatment lasted for eight weeks. During the period of the experiment, trained and skilled animal technicians undertaken monitoring observations at least twice daily to minimize the pain in mice. At the end of the experiment, all mice were fasted for 12 h but had free access to water and then euthanized. Blood samples were collected and centrifuged to obtain serum at 5,000×*g* for 15 min at 4℃. The liver and heart tissues were immediately removed and washed with pre-cooled phosphate buffer saline (PBS) (Gibco, Thermo Fisher Scientific, Grand Island, NY, USA). A 1×1 cm^2 dorsal skin was collected from each mouse after hair removal. The contents of the small intestine and colon were collected separately on ice. All samples were stored at -80℃ until further analysis within two months.

■ **Determination of the content of hydroxyproline and hyaluronic acid in the skin**
The skin sample was cut into about 2×2 mm^2 pieces and then ground into powder using a mortar under liquid nitrogen. Subsequently, the skin sample was treated with acetone-diethyl ether (1:1, *v/v*) to remove lipids. After drying, a 20 mg tissue sample was collected and then the content of hydroxyproline and hyaluronic acid was determined using a mouse hydroxyproline ELISA kit and a mouse hyaluronic acid ELISA kit, respectively, according to the manufacturer's instructions (Jiangsu Meimian Biotech., Yancheng, China).

■ **Anti-oxidant enzyme activity and MDA content assays**
The activities of SOD, GSH-Px, and the level of MDA in serum were determined using a SOD assay kit (WST-1 method), a GSH-PX assay kit (colorimetric method), and an MDA assay kit (thiobarbituric acid method), respectively, according to the manufacturer's instructions (Nanjing Jiancheng Bioengineering Institute, Nanjing, China). Additionally, 10% (*w/v*) liver and heart tissue PBS homogenates were prepared by tissue grinder (TissueLyser LT, QIAGEN, Hilden, Germany), and then supernatants were obtained by centrifugation (5,000×*g* for 15 min at 4℃), respectively. After protein quantification in supernatants by BCA kit (CoWin Biosciences, Beijing, China), the activities of SOD, GSH-Px and the levels of MDA were determined according to the kit manufacturer's instructions (Nanjing Jiancheng Bioengineering Institute).

■ Cytokine concentration assay in serum
The concentration of IL-1β and TNF-α in serum was measured according to the instructions of mouse IL-1β and TNF-α ELISA kits (Jiangsu Meimian Biotech.).

■ **Measurement of pH and determination of the content of short-chain fatty acids in the gastrointestinal tract**
The samples of the contents of the small intestine and colon were thawed and then diluted with pure neutral water in a ratio of 1:1 (*w/v*). The pH of the solution was measured with a pH meter (FE28, Mettler Toledo, Columbus, OH, USA). SCFAs contents in the small intestine and colon contents were determined using gas chromatography mass spectrometry (GC-MS) as previously reported [Zhao *et al.*, 2018] with slight modification. Briefly, 100 mg of intestinal contents were homogenized with 1.5 mL of phosphate buffer (pH 7.4) and centrifuged. One mL of supernatant was acidified by adding 0.5 mL of 50% (*v/v*) sulfuric acid. Then, organic extraction was performed by adding 2 mL of diethyl ether, followed by vortexing and centrifugation at 5,000×*g* for 5 min. The supernatants, after filtering by 0.22 μm membrane, were analyzed using the GC-MS system (GC-2010PLUS, Shimadzu, Kyoto, Japan) with a DB-FATWAX capillary column (30 m×0.25 mm, Agilent). Acetic, propionic, isobutyric, *n*-butyric, isovaleric, and *n*-valeric acids were used as standards (Macklin Biochemical Co., Shanghai, China). GC conditions: initial temperature 120℃ maintained for 2 min, then heating up to 140℃ at 5℃/min, held for 3 min, finally enhanced to 170℃ at 10℃/min, kept for 5 min; the detector temperature was set at 250℃, the split ratio was 25:1, and the flow rate was 1.8 mL/min.

■ **Statistical analysis**
Data were expressed as mean ± standard deviation. The statistical differences between the groups of *in vivo* experiment were calculated using one-way analysis of variance (ANOVA) with Tukey's test using SPSS 22.0 (IBM Corp., Armonk, NY, USA). The differences were considered significant at *p*<0.05.

RESULTS AND DISCUSSIONS
■ **Structure analysis**
The carbohydrate content of high molecular weight polysaccharide (HM) of *T. fuciformis* fruiting body was 92.5 g/100 g dry weight. The degraded HM (MM) and highly degraded HM (LM) contained 93.1 and 93.5 g carbohydrates/100 g dry weight, respectively. The GC chromatogram of HM after its acid hydrolysis is shown in Figure 1A. The monosaccharide composition of HM mainly consisted of mannose, fucose, xylose, and glucose in a molar ratio of 4.14:0.98:0.81:0.62, which was estimated from the peak areas. A small amount of glucuronic acid and arabinose was also found in the HM sample. In the ^{1}H NMR spectrum of HM, the peaks in the range of δ 4.3–5.9 ppm (Figure 1 B) were the chemical shifts of the anomeric hydrogen in the sugar ring [Agrawal, 1992]. The peaks at δ 5.57, 5.41, 5.20, and 5.13 ppm demonstrated α-configuration in the polysaccharide molecules, while the peaks at δ 4.53, 4.51, and 4.40 ppm indicated β-configuration. In the ^{13}C NMR spectrum, multiple peaks
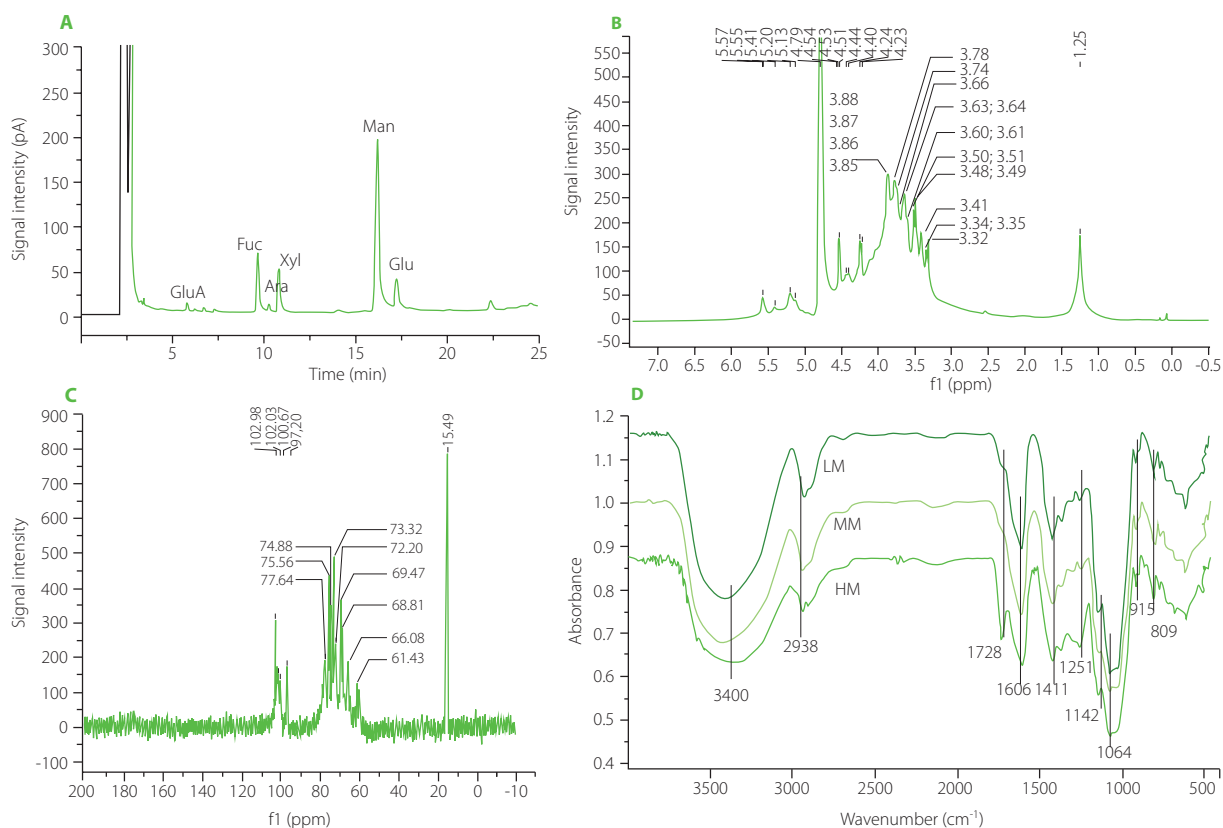
Figure 1. Results of structure analysis of high molecular weight *Tremella fuciformis* polysaccharide (HM), degraded HM (MM) and highly degraded HM (LM). (**A**) Gas chromatography separation of monosaccharides of HM after its hydrolysis; (**B**) ¹H NMR spectrum of HM; (**C**) ¹³C NMR spectrum of HM; (**D**) Fourier-transform infrared spectra of HM, MM, and LM. GluA, glucuronic acid; Rha, rhamnose; Fuc, fucose; Ara, arabinose; Xyl, xylose; Man, mannose; Gal, galactose; Glu, glucose.

in the range of 95.00–110.00 ppm belonged to anomeric carbon signals [Agrawal, 1992], indicating that HM was composed of several monosaccharides (Figure 1C). Specifically, four peaks at δ102.98(C1), 102.03(C1), 100.67(C1), and 97.20(C1) ppm suggested the presence of four types of monosaccharides in the backbone chain of HM [Hu *et al.*, 2016], which was consistent with the results of GC-MS.

The FT-IR spectra of the HM, MM and LM samples showed similar infrared absorption profiles (Figure 1D). Characteristic peaks of the FT-IR spectra were presented at approximately 3,400; 2,938; 1,606; 1,411; 1,142; 1,064; 915, and 809 cm⁻¹. Absorption peaks were observed at 3,400 and 2,938 cm⁻¹ due to the stretching vibration of O-H [Chen *et al.*, 2020] and C-H [Jeong *et al.*, 2019], respectively. The peak at 1,606 cm⁻¹ is attributed to the bound water in the samples [Velazquez *et al.*, 2003]. Absorption bands in the region of 1,200-1,000 cm⁻¹ are typical for polysaccharide molecules due to the stretching vibration of C-O, C-C, and the angular vibration of C-O-H [Barker *et al.*, 1954]. The peak at 915 cm⁻¹ indicates the presence of ᴅ-glucopyranosyl [Zhang *et al.*, 2013], and the peak at 809 cm⁻¹ suggests the presence of α-ᴅ-mannopyranose in molecules [Wang *et al.*, 2015; Zhang *et al.*, 2013]. These results indicated that US/H₂O₂ treatment did not affect the major functional groups of TFPs.

In the HPGPC chromatograms of HM, MM and LM (Figure 2A–C), the large peak before the retention time of 20 min belongs to TFPs, and the small peak after 25 min is attributed to

the used solvent. HM exhibited a narrow peak, while both MM and LM showed wide peaks, suggesting that US/H₂O₂ treatment reduced the uniformity of polysaccharide molecules. The retention time of the peak for HM, MM, and LM was 13.26, 14.59, and 18.91 min, respectively, corresponding to a molecular weight of 58.3×10^6, 4.68×10^6, and 3.14×10^5 Da, elucidating a gradual approximately 10-fold reduction in the average molecular weight for the three TFPs. Further, the conformation was measured by Congo red method. The maximum absorption wavelength (λ_{max}) of all TFPs solutions gradually declined with increasing NaOH concentration (0–0.5 M), similar to the feature of the Congo red solution (Figure 2D). There was no noticeable shift of λ_{max} in TFPs solutions, demonstrating the absence of triple helix conformation in all TFPs samples. On the contrary, the obvious shift of λ_{max} in yeast β-glucan solution demonstrated that triple helix β-glucan-Congo red complexes formed in the solution.

As a result, HM was found to be novel heteropolysaccharide derived from the fruiting body of *T. fuciformis* based on the monosaccharide composition and the molecular weight distribution, which exhibited a larger molecular weight than previously reported ones [Wu *et al.*, 2019; Yang *et al.*, 2019]. The possible reason for this, besides the resource and purification method, might be the differences in the drying process of the fruiting body of *T. fuciformis* [Lin & Tsai, 2019]. By a combined method of US/H₂O₂ treatment, two TFPs with gradient-decreased molecular weight were prepared successfully. Because US/H2O₂ treatment did not
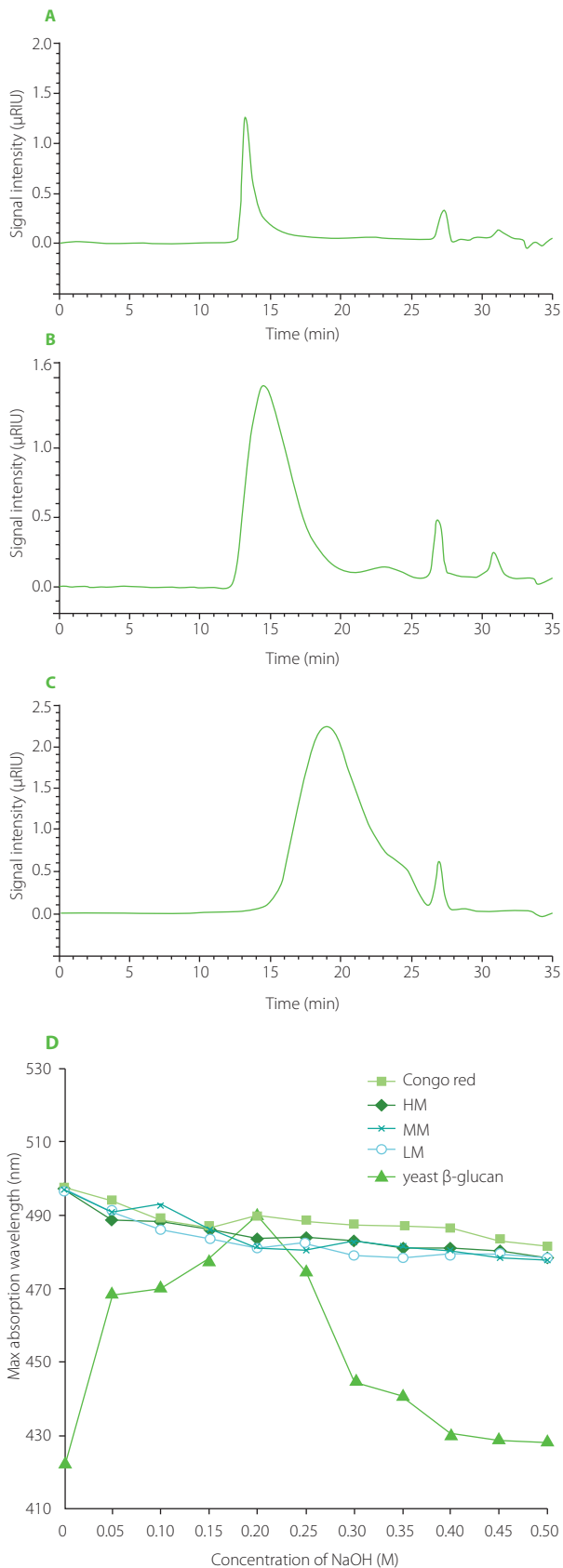
Figure 2. Molecular weight distribution and results of conformation analysis of high molecular weight *Tremella fuciformis* polysaccharide (HM), degraded HM (MM) and highly degraded HM (LM). High-performance gel permeation chromatography (HPGPC) of HM (**A**), MM (**B**), and LM (**C**). (**D**) Maximum absorption wavelength of Congo red solution with polysaccharides and yeast β-glucan at different concentrations of NaOH.

change the primary structures of TFPs, such as monosaccharide composition and glycosidic linkages in the main backbone [Li *et al.*, 2020], therefore, the following anti-oxidant and anti-aging experiments using the three TFPs could mainly focus on the effects of polysaccharides with different molecular weights on bioactivity.

■ **Anti-oxidant activity *in vitro***

As shown in Figure 3, the scavenging activity against DPPH radical, hydroxyl radical, and superoxide anion radical exhibited a concentration-dependent manner and ranged from 5.86 to 14.67% for HM, 2.75 to 11.52% for MM, and 4.75 to 18.95% for LM, respectively, although significantly higher values were determined for AA. Notably, the radical scavenging activity of the three samples also displayed a molecular weight-dependent manner, except for superoxide anion radical when TFPs were applied at a concentration of 150 µg/mL. Specifically, the radical scavenging activity decreased in a sequence of LM, MM, and HM. Unsurprisingly, LM showed the best anti-oxidant activities among the three TFPs. This was consistent with the previous findings that polysaccharides with low molecular weight have higher anti-oxidant activity than those with high molecular weight [Li *et al.*, 2020; Ogutu & Mu, 2017]. Possible reasons might be that polysaccharides with lower molecular weight contained more polysaccharide fractions under the same concentration, which resulted in more hydroxyl groups in molecules being exposed to free radicals in solutions, leading to a higher scavenging activity against radicals [Li *et al.*, 2020; Wu *et al.*, 2018].

■ **Effects of TFPs on D-galactose-induced aging mice**
■ Skin anti-aging activity

During the experimental period, the mice in the Normal group moved flexibly with shiny fur. In contrast, the mice in the Model group were inactive, with fur dull and messy. The behavior and the fur color of the mice improved obviously in the TFPs--treated groups, compared with the Model group. The body weight of the mice in all groups increased gradually and no statistically significant differences were observed between the groups (data not shown). To assess the degree of skin aging, the content of hydroxyproline and hyaluronic acid was evaluated in five groups. As presented in Figure 4, the content of hydroxyproline and hyaluronic acid was extremely lower in the Model group than in the Normal group ($p<0.01$), demonstrating that eight--week treatment with D-galactose substantially accelerated skin aging in mice. Treatments with HM, MM, and LM obviously increased the content of hydroxyproline in the skin by 91.9, 101.4, and 94.6%, respectively, compared with the Model group ($p<0.01$). Similarly, administrations of HM, MM, and LM also greatly improved the content of hyaluronic acid by 34.3, 103.3, and 73.4%, respectively, compared with the Model group ($p<0.01$). These results further confirmed the anti-aging effects of TFPs reported in previous studies [Wen *et al.*, 2016; Zhang *et al.*, 2014]. In particular, MM displayed the best performance in ameliorating the loss of hydroxyproline and hyaluronic acid induced by D-galactose treatment among the three samples.

A

B

C
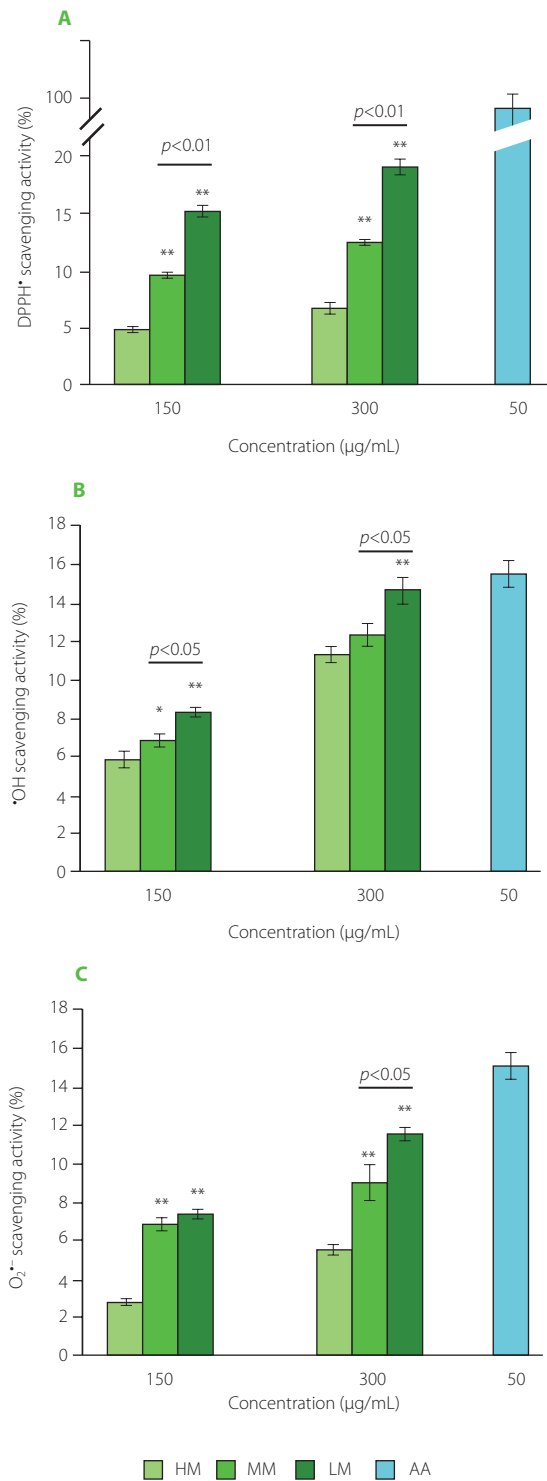
Figure 3. Scavenging activities of high molecular weight *Tremella fuciformis* polysaccharide (HM), degraded HM (MM) and highly degraded HM (LM) against DPPH radical (**A**), hydroxyl radical (**B**), and superoxide anion radical (**C**). AA, ascorbic acid. *, ** represent *p*<0.05, and *p*<0.01, respectively, compared with the HM at the same concentration.

■ **Anti-oxidative stress parameters**

In comparison with the Normal group, as shown in Figure 5, treatment with D-galactose substantially decreased the activities of SOD and GSH-Px (*p*<0.01) and dramatically promoted the production of MDA (*p*<0.01) in serum, liver, and heart tissues in mice in the Model group. These results further

A

B
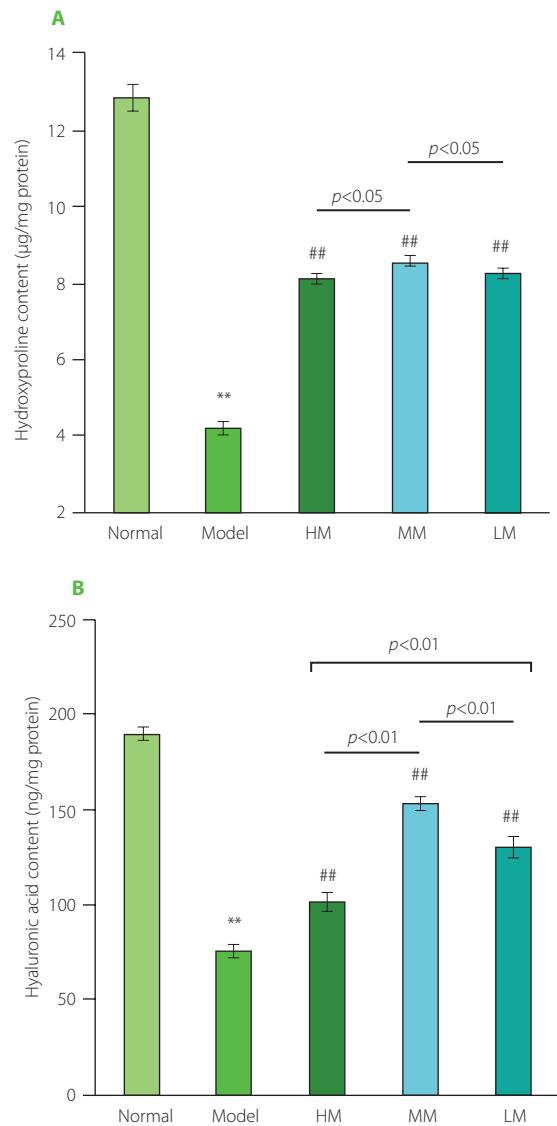
Figure 4. The contents of hydroxyproline (**A**) and hyaluronic acid (**B**) in the skin of D-galactose-induced aging mice treated with high molecular weight *Tremella fuciformis* polysaccharide (HM), degraded HM (MM) and highly degraded HM (LM). *, ** represent *p*<0.05, *p*<0.01, respectively, compared with the Normal group; #, ## represent *p*<0.05, *p*<0.01, respectively, compared with the Model group.

elucidated that the aging mouse model was established successfully. Notably, three TFPs samples significantly improved the activities of SOD and GSH-Px in serum, liver, and heart tissues in D-galactose-treated mice (*p*<0.05 or *p*<0.01), except for the activity of SOD in heart in the HM group and the activity of GSH-Px in serum in the HM and LM groups. Correspondingly, the level of MDA obviously decreased in serum, liver, and heart tissues in three groups (*p*<0.05 or *p*<0.01) except for liver tissue in the HM group. These results demonstrated that all tested TFPs could mitigate oxidative stress in D-galactose-induced aging mice. Particularly, MM showed the highest efficacy in relieving oxidative stress among the three TFPs.

Notably, the degree of amelioration of skin aging, evidenced by the increased contents of hydroxyproline and hyaluronic acid in the skin, was consistent with the reduction of oxidative stress induced by the three TFPs. This further demonstrated that
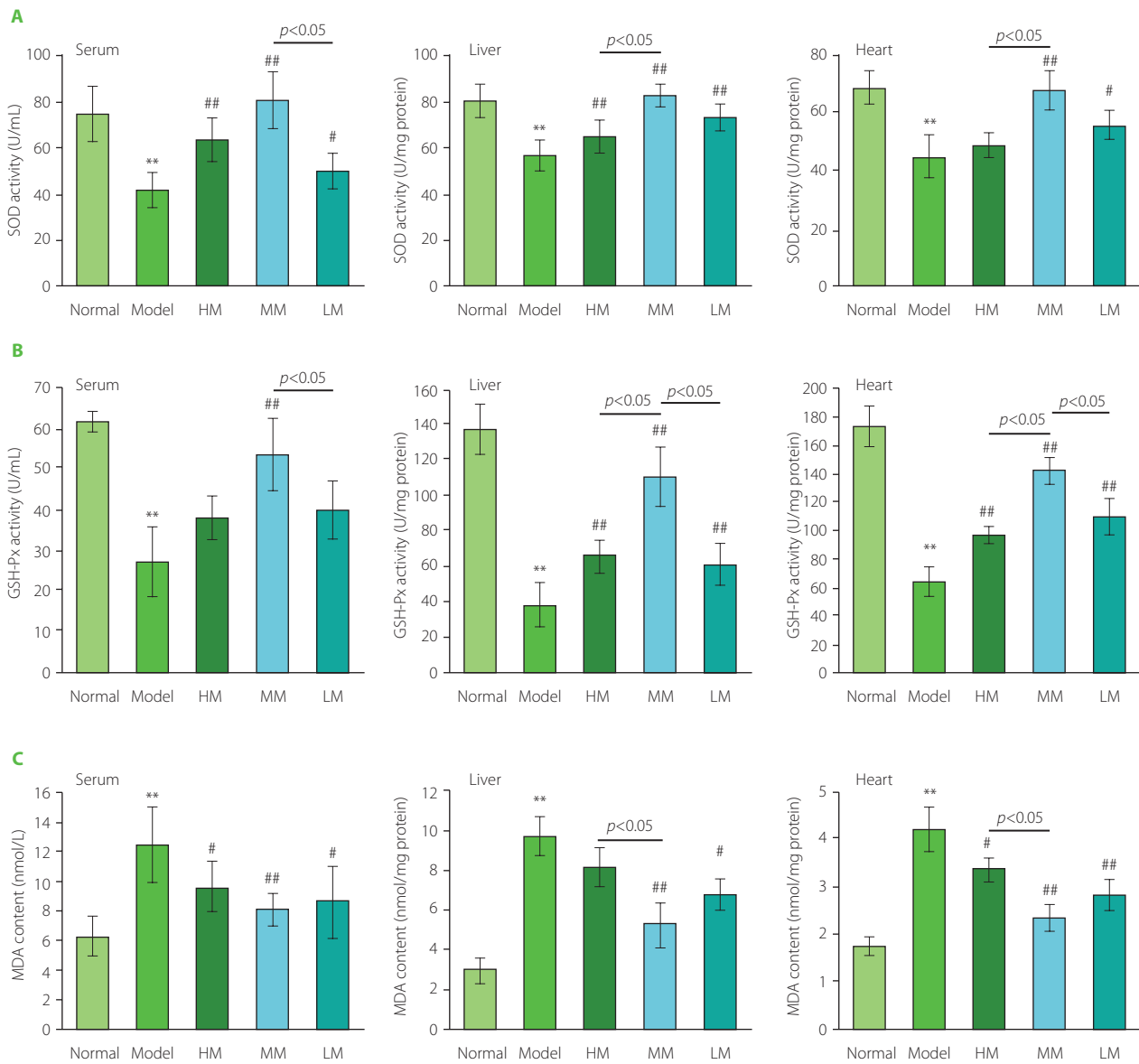
Figure 5. The activities of superoxide dismutase (SOD) (**A**), glutathione peroxidase (GSH-Px) (**B**), and the level of malondialdehyde (MDA) (**C**) in serum, liver, and heart in D-galactose-induced aging mice treated with high molecular weight *Tremella fuciformis* polysaccharide (HM), degraded HM (MM) and highly degraded HM (LM). *, ** represent $p<0.05$, $p<0.01$, respectively, compared with the Normal group; #, ## represent $p<0.05$, $p<0.01$, respectively, compared with the Model group.

the ameliorating effect of TFPs on skin aging could be partially attributed to the improvement in the activity of anti-oxidant enzymes [Wen *et al.*, 2016]. Antioxidants (*e.g.*, polyphenols) provide anti-oxidant protection against oxidative damage *in vivo* by regulating complicated intracellular signals for induction of anti--oxidant enzymes [Forman *et al.*, 2014; Forman & Zhang, 2021]. The nuclear factor erythroid 2-like 2 (Nrf2) is a critical regulator of anti-oxidative responses in intracellular signaling pathways [Vomund *et al.*, 2017]. Nrf2/antioxidant response element (ARE) signaling pathway plays key roles in maintaining intracellular redox homeostasis [Saha *et al.*, 2020]. In a recent study, *Grifola frondose--*derived polysaccharides elevated anti-oxidative capacity in an acute liver injury mouse model by regulating the Nrf2/ARE signaling pathway [Meng *et al.*, 2021]. These results provide new clues for revealing the molecular mechanisms underlying the anti-oxidant activities of TFPs *in vivo*. Further studies are needed to demonstrate

the molecular mechanism and the correlation between the molecular weight of polysaccharides and the expression profiles of anti-oxidant genes in the mammalian model.

■ **Anti-inflammatory activity**

As shown in Figure 6, the levels of IL-1β and TNF-α substantially increased in the Model group by 2.45 and 3.01 times, respectively, compared with the Normal group, indicating a high level of inflammation in D-galactose-induced aging mice. The levels of IL-1β and TNF-α in all three TFPs-treated groups were lower than those in the Model group ($p<0.01$), demonstrating the excellent anti-inflammatory activity of the samples tested. Specifically, the order of the anti-inflammatory activity of the three TFPs samples was MM, LM, and HM. MM showed the best anti-inflammatory activity among the three TFPs, demonstrating an important role of molecular weight in influencing bioactivity
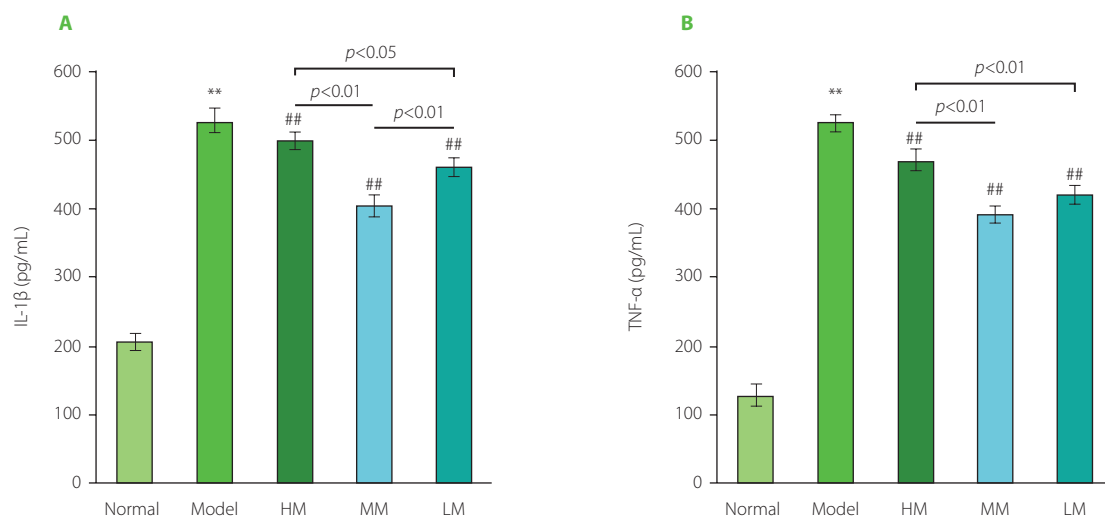
Figure 6. The levels of interleukin 1β (IL-1β) (**A**) and tumor necrosis factor α (TNF-α) (**B**) in serum of ᴅ-galactose-induced aging mice treated with high molecular weight *Tremella fuciformis* polysaccharide (HM), degraded HM (MM) and highly degraded HM (LM). ** represent $p<0.01$, compared with the Normal group; ## represent $p<0.01$, compared with the Model group.

for mushroom polysaccharides. Pretreatment with TFPs could attenuate lipopolysaccharide (LPS)-induced oxidative stress and inflammation by inhibiting nuclear factor κB (NF-κB) activation through downregulating miR-155 expression, one of the key small RNAs regulating NF-κB activation, in RAW264.7 macrophages [Ruan *et al.*, 2018]. Numerous studies have documented that mushroom polysaccharides and their metabolites produced by gut microbiota, such as SCFAs, display anti-inflammatory activities through multiple pathways, including modulation of immune cell receptor-involved NF-κB signaling pathway and promotion of the proliferation and differentiation of Foxp3+ regulatory T-cells [Liu *et al.*, 2022]. Given the diverse structures of TFPs [Wu *et al.*, 2019], the low absorption rate of TFPs through oral administration route (only 0.4% in rat) [Gao *et al.*, 2002], and the complexity of gut microbiota in the metabolism of polysaccharides [Song *et al.*, 2021], there remain complex challenges in fully understanding the molecular mechanism of anti-inflammatory activity of TFPs *in vivo*. However, efforts need to be undertaken in future work.

Matrix metalloproteinases (MMPs) can degrade a variety of components of the extracellular matrix (ECM), such as collagen and hyaluronic acid [Chen *et al.*, 2013]. Higher levels of MMPs are observed in aged human skin, and MMPs play an important role in the remodeling of ECM in skin aging [Shin *et al.*, 2019]. Inflammation increases the levels of MMPs in the vascular wall and plasma of obese women [Ozen *et al.*, 2019], suggesting an association between the level of inflammation and the level of MMPs. Mechanically, the activation of activator protein 1 (AP-1) and NF-κB-related intracellular signaling pathways increases the expression of MMPs [Shin *et al.*, 2019], indicating that overproduction of reactive oxygen species (ROS) and a high level of pro-inflammatory cytokines would promote the levels of MMPs. TFPs could inhibit NF-κB activation under inflammatory status in cells [Ruan *et al.*, 2018]. As a theoretical speculation, TFPs might regulate the level of MMPs in aging mice

via the inactivation of NF-κB-related signaling pathway, leading to a decreased level of MMPs in the skin. In the present study, the degree of amelioration in the loss of hydroxyproline and hyaluronic acid in the aging skin was positively associated with the reduction of inflammatory cytokine levels. This further indicated that the anti-skin aging effect of TFPs, evidenced by amelioration in the loss of hydroxyproline and hyaluronic acid in the skin, might be partially attributed to their anti-inflammatory actions. Further animal experiments should be considered in future studies to elucidate the molecular mechanism of TFPs in modulating MMPs expression.

■ **Alterations in pH and SCFAs production in the gut**

To investigate the responses of the gastrointestinal environment to TFPs treatment, the pH and content of SCFAs (acetic acid, propionic acid, *n*-butyric acid, isobutyric acid, *n*-valeric acid, and isovaleric acid) were determined. As shown in Figure 7A and 7B, the pH in the small intestine was weakly alkaline, while the pH in the colon was slightly acidic. There was no statistical difference ($p≥0.05$) in pH in the small intestinal environment among the five groups. On the contrary, in the colon, the pH in the Model group was lower than that in the Normal group ($p<0.01$), suggesting alterations in microbial metabolites in the colonic environment in ᴅ-galactose-treated mice. TFPs treatments differentially reversed the decrease in pH in the colon in ᴅ-galactose-treated mice. Interestingly, the pH in the HM group increased significantly (6.50 *vs*. 5.92, $p<0.01$), compared with the Model group. Notably, the pH was higher in the HM group than in the LM group ($p<0.05$), suggesting the differential impacts of the three TFPs on gut microbial metabolism.

Furthermore, almost no SCFAs were detected in the small intestinal contents in all mice. By contrast, acetic acid and propionic acid were the predominant SCFAs in the colon, followed by *n*-butyric acid (Figure 7D). An unexpected increase in the amount of total SCFAs was observed in the Model group ($p<0.01$,
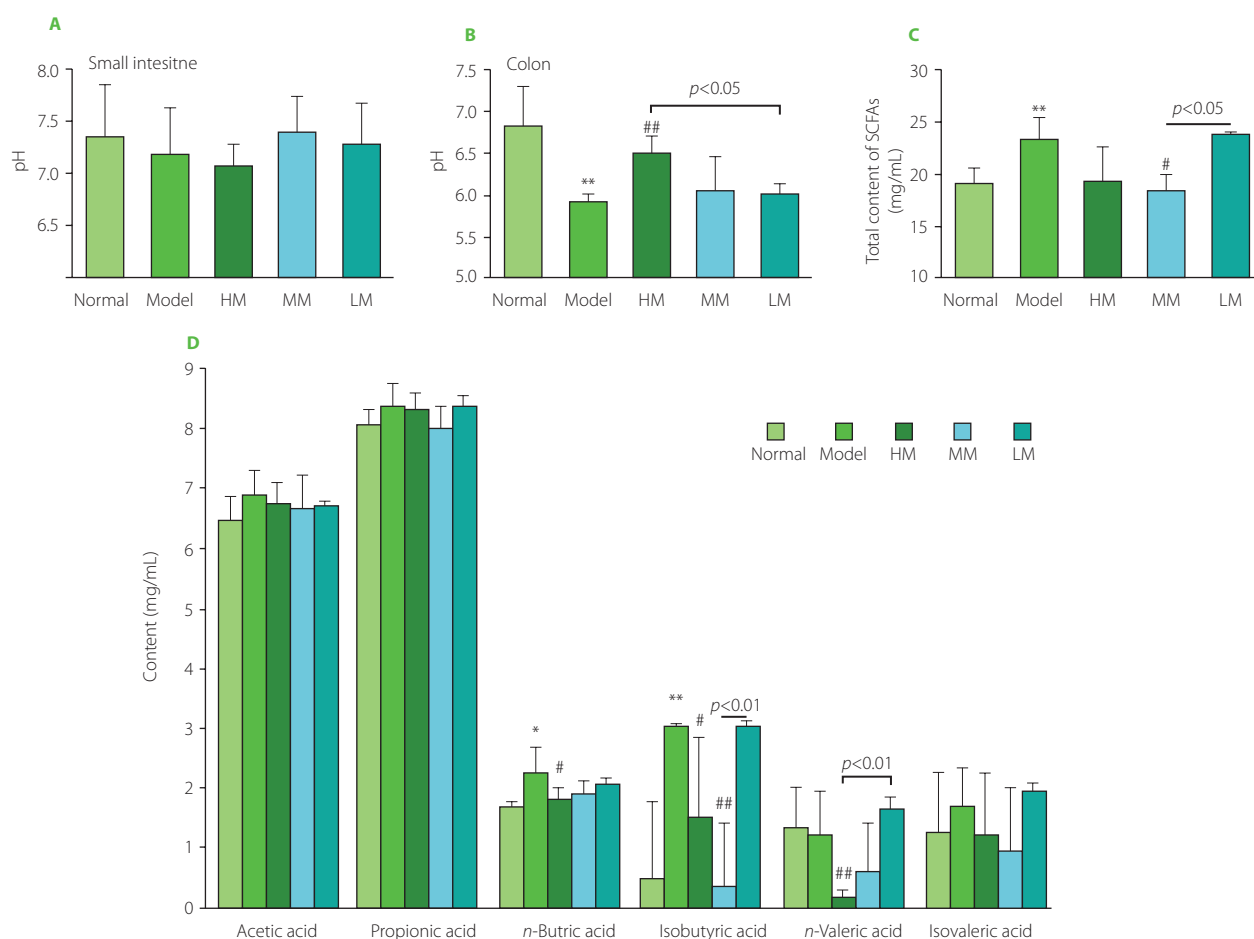
Figure 7. Values of pH in the small intestine (**A**) and colon (**B**), and the total amount of short-chain fatty acids (SCFAs) (**C**) and the production of individual SCFAs in the colon of D-galactose-induced aging mice treated with high molecular weight *Tremella fuciformis* polysaccharide (HM), degraded HM (MM) and highly degraded HM (LM). *, ** represent $p<0.05$, $p<0.01$, respectively, compared with the Normal group; #, ## represent $p<0.05$, $p<0.01$, respectively, compared with the Model group.

Figure 7C). Notably, the amount of total SCFAs in the HM and MM groups decreased, compared with the Model group, whereas the amount of total SCFAs in the LM group was equivalent to that in the Model group. These observations indicated that TFPs with different molecular weights might preferentially be utilized by different SCFAs-producing bacteria and, therefore, exert differential impacts on the colonic microbial metabolism. In previous studies, a decrease in the contents of SCFAs in feces in mice, as well as reduced richness and diversity of the gut microbiota, was induced by D-galactose treatment [Zhang J. *et al.*, 2017; Zhang Z. *et al.*, 2020]. The opposite results of SCFAs production in the current study might be attributed to the differences in housing environments and mouse species, since environmental factors and genetic background strongly influence the composition of gut microbiota [Ericsson *et al.*, 2018]. More investigations are needed to clarify the relationship between the changes in SCFAs production and the progress of aging.

In detail, among the individual SCFAs, the contents of *n*-butyric acid and isobutyric acid in the Model group increased significantly ($p<0.05$ and $p<0.01$), whereas the others did not change obviously, compared with the Normal group (Figure 7D). However, HM and MM treatments markedly reversed the abnormal increases in *n*-butyric acid and isobutyric acid

production in D-galactose-treated mice. In particular, the contents of isobutyric acid in the MM group and *n*-valeric acid in the HM group were dramatically decreased compared with those of the Model and LM groups. The inconsistent profiles of the SCFAs in three groups indicated the complicated impacts of TFPs with different structures on microbial metabolism.

Generally, mushroom polysaccharides can modulate gut microbial composition and increase SCFAs-producing bacteria, leading to increased contents of SCFAs in the gut [Li *et al.*, 2021]. Conversely, HM and MM treatments induced a decrease in the amount of total SCFAs. These phenomena suggested that the contents of SCFAs in the gut might vary in a physiological range for a healthy host. For example, an increased total content of SCFAs in the obese subjects was reported compared to the lean ones [Schwiertz *et al.*, 2010]. TFPs might modulate gut microbial community to maintain gut homeostasis through direct and indirect routes. On the one hand, TFPs might reverse the abnormal increase in contents of SCFAs induced by D-galactose treatment through directly modulating the intestinal microbiota due to the prebiotic properties of mushroom polysaccharides [Li *et al.*, 2021]; on the other hand, TFPs could stimulate intestinal mucosal immune responses which, in turn, shape the intestinal microbial composition, resulting in a restoration of the contents of SCFAs. Recent experimental

evidence revealed the bioactive properties of TFPs in the restoration of the gut microbiota in dextran sodium sulfate (DSS)-induced colitis model [Xiao *et al.*, 2021; Xu *et al.*, 2021], as well as the direct anti-inflammatory activity *in vitro* [Ruan *et al.*, 2018; Xiao *et al.*, 2021], suggesting the dual roles of TFPs in modulating gut microbiota. Additionally, oat β-glucan with a lower average molecular weight exhibited a higher production of SCFAs in the *in vitro* gut fermentation model [Dong *et al.*, 2020], partially explaining that LM induced the highest production of SCFAs in the gut among the three TFPs samples. However, well-designed experiments, such as those using a germ-free mouse model and gut microbiota transplantation technology, are urgently needed to reveal whether the alterations in gut microbiota composition and metabolites are a consequence of mushroom polysaccharide interventions or a cause of health benefits of mushroom polysaccharides.

CONCLUSIONS

TFPs with high molecular weight, mainly consisting of mannose, fucose, xylose, and glucose, and two differentially degraded TFPs were obtained from the fruiting body of *T. fuciformis*. Three TFPs with gradient-decreased molecular weight by approximately 10-times, 58.3×10^6, 4.68×10^6, and 3.14×10^5 Da, respectively, showed concentration- and molecular weight-dependent activities in scavenging free radicals *in vitro*. Furthermore, three TFPs effectively relieved aging features in D-galactose-induced aging mice, as evidenced by amelioration of the loss of hydroxyproline and hyaluronic acid in the skin, increased activities of GSH-Px and SOD, and decreased levels of MDA in the serum, liver, and heart tissues, reduced levels of inflammatory cytokines in the serum, and partial restoration of the alterations in pH and SCFAs production in the colon. Particularly, TFPs with the medium molecular weight exhibited the best performance in ameliorating skin aging, reducing oxidative stress, and anti-inflammation. These results not only confirmed the antioxidant activity of TFPs, but more importantly revealed a preliminary relationship between molecular weight and anti-aging activity of TFPs *in vivo*.

RESEARCH FUNDING

ACKNOWLEDGEMENTS

CONFLICT OF INTERESTS

The authors declare no conflicts of interest.

ORCID IDS

J. Guan   https://orcid.org/0009-0008-6865-4162
Y. Hua   https://orcid.org/0009-0008-6466-331X
G. Jiang   https://orcid.org/0009-0009-4694-0579
X. Liu   https://orcid.org/0009-0005-6249-4194
D. Luo   https://orcid.org/0000-0002-8584-7344
X. Xu   https://orcid.org/0000-0001-9177-9723
X. Zhang   https://orcid.org/0009-0000-7947-138X

REFERENCES

1. Agrawal, P.K. (1992). NMR spectroscopy in the structural elucidation of oligosaccharides and glycosides. *Phytochemistry*, *31*(10), 3307–3330.
https://doi.org/10.1016/0031-9422(92)83678-R

2. Barker, S.A., Bourne, E.J., Stacey, M., Whiffen, D.H. (1954). Infra-red spectra of carbohydrates. Part I. Some derivatives of D-glucopyranose. *Journal of the Chemical Society (Resumed)*, 171–176.
https://doi.org/10.1039/jr9540000171

3. Cao, S., Zhan, H., Fu, S., Chen, L. (2007). Regulation of superoxide anion radical during the oxygen delignification process. *Chinese Journal of Chemical Engineering*, *15*(1), 132–137.
https://doi.org/10.1016/S1004-9541(07)60046-9

4. Chen, Q., Jin, M., Yang, F., Zhu, J., Xiao, Q., Zhang, L. (2013). Matrix metalloproteinases: Inflammatory regulators of cell behaviors in vascular formation and remodeling. *Mediators of Inflammation*, *2013*, art. no. 928315.
https://doi.org/10.1155/2013/928315

5. Chen, X., Zhang, R., Li, Y., Li, X., You, L., Kulikouskaya, V., Hileuskaya, K. (2020). Degradation of polysaccharides from *Sargassum fusiforme* using UV/H_2O_2 and its effects on structural characteristics. *Carbohydrate Polymers*, *230*, art. no. 115647.
https://doi.org/10.1016/j.carbpol.2019.115647

6. Dong, J.L., Yang, M., Zhu, Y.Y., Shen, R.L., Zhang, K.Y. (2020). Comparative study of thermal processing on the physicochemical properties and prebiotic effects of the oat β-glucan by *in vitro* human fecal microbiota fermentation. *Food Research International*, *138*(Part B), art. no. 109818.
https://doi.org/10.1016/j.foodres.2020.109818

7. Ericsson, A.C., Gagliardi, J., Bouhan, D., Spollen, W.G., Givan, S.A., Franklin, C.L. (2018). The influence of caging, bedding, and diet on the composition of the microbiota in different regions of the mouse gut. *Scientific Reports*, *8*(1), art. no. 4065.
https://doi.org/10.1038/s41598-018-21986-7

8. Ferreira, S.S., Passos, C.P., Madureira, P., Vilanova, M., Coimbra, M.A. (2015). Structure–function relationships of immunostimulatory polysaccharides: A review. *Carbohydrate Polymers*, *132*, 378–396.
https://doi.org/10.1016/j.carbpol.2015.05.079

9. Forman, H.J., Davies, K.J.A., Ursini, F. (2014). How do nutritional antioxidants really work: Nucleophilic tone and para-hormesis *versus* free radical scavenging *in vivo*. *Free Radical Biology and Medicine*, *66*, 24–35.
https://doi.org/10.1016/j.freeradbiomed.2013.05.045

10. Forman, H.J., Zhang, H. (2021). Targeting oxidative stress in disease: promise and limitations of antioxidant therapy. *Nature Reviews Drug Discovery*, *20*(9), 689–709.
https://doi.org/10.1038/s41573-021-00233-1

11. Gao, Q., Chen, H., Wang, K., Shen, Y. (2002). Studies on the absorption, distribution and clearance of *Tremella* polysaccharide in rats. *Chinese Pharmaceatical Journal*, *37*(3), 205–208.

12. Ge, X., Huang, W., Xu, X., Lei, P., Sun, D., Xu, H., Li, S. (2020). Production, structure, and bioactivity of polysaccharide isolated from *Tremella fuciformis* XY. *International Journal of Biological Macromolecules*, *148*, 173–181.
https://doi.org/10.1016/j.ijbiomac.2020.01.021

13. Heinrich, M., Appendino, G., Efferth, T., Fürst, R., Izzo, A.A., Kayser, O., Pezzuto, J.M., Viljoen, A. (2020). Best practice in research – Overcoming common challenges in phytopharmacological research. *Journal of Ethnopharmacology*, *246*, art. no. 112230.
https://doi.org/10.1016/j.jep.2019.112230

14. Hu, P., Li, Z., Chen, M., Sun, Z., Ling, Y., Jiang, J., Huang, C. (2016). Structural elucidation and protective role of a polysaccharide from *Sargassum fusiforme* on ameliorating learning and memory deficiencies in mice. *Carbohydrate Polymers*, *139*, 150–158.
https://doi.org/10.1016/j.carbpol.2015.12.019

15. Huang, S.Q., Li, J.W., Li, Y.Q., Wang, Z. (2011). Purification and structural characterization of a new water-soluble neutral polysaccharide GLP-F1-1 from *Ganoderma lucidum*. *International Journal of Biological Macromolecules*, *48*(1), 165–169.
https://doi.org/10.1016/j.ijbiomac.2010.10.015

16. Huang, X., Nie, S. (2015). The structure of mushroom polysaccharides and their beneficial role in health. *Food Function*, *6*(10), 3205–3217.
https://doi.org/10.1039/C5FO00678C

17. Jeong, H.K., Lee, D., Kim, H.P., Baek, S.H. (2019). Structure analysis and antioxidant activities of an amylopectin-type polysaccharide isolated from dried fruits of *Terminalia chebula*. *Carbohydrate Polymers*, *211*, 100–108.
https://doi.org/10.1016/j.carbpol.2019.01.097

18. Lee, H.H., Lee, J.S., Cho, J.Y., Kim, Y.E., Hong, E.K. (2009). Structural characteristics of immunostimulating polysaccharides from *Lentinus edodes*. *Journal of Microbiology and Biotechnology*, *19*(5), 455–461.
https://doi.org/10.4014/jmb.0809.542

19. Li, M., Ma, F., Li, R., Ren, G., Yan, D., Zhang, H., Zhu, X., Wu, R., Wu, J. (2020). Degradation of *Tremella fuciformis* polysaccharide by a combined ultra-

sound and hydrogen peroxide treatment: Process parameters, structural characteristics, and antioxidant activities. *International Journal of Biological Macromolecules*, *160*, 979–990.
https://doi.org/10.1016/j.ijbiomac.2020.05.216

20. Li, M., Yu, L., Zhao, J., Zhang, H., Chen, W., Zhai, Q., Tian, F. (2021). Role of dietary edible mushrooms in the modulation of gut microbiota. *Journal of Functional Foods*, *83*, art. no. 104538.
https://doi.org/10.1016/j.jff.2021.104538

21. Lin, C.P., Tsai, S.Y. (2019). Differences in the moisture capacity and thermal stability of *Tremella fuciformis* polysaccharides obtained by various drying processes. *Molecules*, *24*(15), art. no. 2856.
https://doi.org/10.3390/molecules24152856

22. Liu, J., Luo, J., Ye, H., Sun, Y., Lu, Z., Zeng, X. (2009). Production, characterization and antioxidant activities *in vitro* of exopolysaccharides from endophytic bacterium *Paenibacillus polymyxa* EJS-3. *Carbohydrate Polymers*, *78*(2), 275–281.
https://doi.org/10.1016/j.carbpol.2009.03.046

23. Liu, X., Luo, D., Guan, J., Chen, J., Xu, X. (2022). Mushroom polysaccharides with potential in anti-diabetes: Biological mechanisms, extraction, and future perspectives: A review. *Frontiers in Nutrition*, *9*, art. no. 1087826.
https://doi.org/10.3389/fnut.2022.1087826

24. Liu, X., Wang, X., Xu, X., Zhang, X. (2019). Purification, antitumor and anti-inflammation activities of an alkali-soluble and carboxymethyl polysaccharide CMP33 from *Poria cocos*. *International Journal of Biological Macromolecules*, *127*, 39–47.
https://doi.org/10.1016/j.ijbiomac.2019.01.029

25. Meng, M., Zhang, R., Han, R., Kong, Y., Wang, R., Hou, L. (2021). The polysaccharides from the *Grifola frondosa* fruiting body prevent lipopolysaccharide/d-galactosamine-induced acute liver injury *via* the miR-122-Nrf2/ARE pathways. *Food and Function*, *12*(5), 1973–1982.
https://doi.org/10.1039/D0FO03327H

26. Ogutu, F.O., Mu, T.H. (2017). Ultrasonic degradation of sweet potato pectin and its antioxidant activity. *Ultrasonics Sonochemistry*, *38*, 726–734.
https://doi.org/10.1016/j.ultsonch.2016.08.014

27. Oliveira, R., Marques, F., Azeredo, J. (1999). Purification of polysaccharides from a biofilm matrix by selective precipitation of proteins. *Biotechnology Techniques*, *13*(6), 391–393.
https://doi.org/10.1023/A:1008954301470

28. Ozen, G., Boumiza, S., Deschildre, C., Topal, G., Longrois, D., Jakobsson, P.J., Michel, J.B., Jacob, M.P., Chahed, K., Norel, X. (2019). Inflammation increases MMP levels via PGE$_2$ in human vascular wall and plasma of obese women. *International Journal of Obesity*, *43*(9), 1724–1734.
https://doi.org/10.1038/s41366-018-0235-6

29. Ruan, Y., Li, H., Pu, L., Shen, T., Jin, Z. (2018). *Tremella fuciformis* polysaccharides attenuate oxidative stress and inflammation in macrophages through miR-155. *Analytical Cellular Pathology*, *2018*, art. no. 5762371.
https://doi.org/10.1155/2018/5762371

30. Saha, S., Buttari, B., Panieri, E., Profumo, E., Saso, L. (2020). An overview of Nrf2 signaling pathway and its role in inflammation. *Molecules*, *25*(22), art. no. 5474.
https://doi.org/10.3390/molecules25225474

31. Schwiertz, A., Taras, D., Schäfer, K., Beijer, S., Bos, N.A., Donus, C., Hardt, P.D. (2010). Microbiota and SCFA in lean and overweight healthy subjects. *Obesity*, *18*(1), 190–195.
https://doi.org/10.1038/oby.2009.167

32. Shin, J.W., Kwon, S.H., Choi, J.Y., Na, J.I., Huh, C.H., Choi, H.R., Park, K.C. (2019). Molecular mechanisms of dermal aging and antiaging approaches. *International Journal of Molecular Sciences*, *20*(9), art. no. 2126.
https://doi.org/10.3390/ijms20092126

33. Song, Q., Wang, Y., Huang, L., Shen, M., Yu, Y., Yu, Q., Chen, Y., Xie, J. (2021). Review of the relationships among polysaccharides, gut microbiota, and human health. *Food Research International*, *140*, art. no. 109858.
https://doi.org/10.1016/j.foodres.2020.109858

34. Velazquez, G., Herrera-Gómez, A., Martín-Polo, M.O. (2003). Identification of bound water through infrared spectroscopy in methylcellulose. *Journal of Food Engineering*, *59*(1), 79–84.
https://doi.org/10.1016/S0260-8774(02)00428-4

35. Venturella, G., Ferraro, V., Cirlincione, F., Gargano, M.L. (2021). Medicinal mushrooms: Bioactive compounds, use, and clinical trials. *International Journal of Molecular Sciences*, *22*(2), art. no. 634.
https://doi.org/10.3390/ijms22020634

36. Vomund, S., Schäfer, A., Parnham, M.J., Brüne, B., von Knethen, A. (2017). Nrf2, the master regulator of anti-oxidative responses. *International Journal of Molecular Sciences*, *18*(12), art. no. 2772.
https://doi.org/10.3390/ijms18122772

37. Wang, H., Cheng, X., Shi, Y., Le, G. (2015). Preparation and structural characterization of poly-mannose synthesized by phosphoric acid catalyzation under microwave irradiation. *Carbohydrate Polymers*, *121*, 355–361.
https://doi.org/10.1016/j.carbpol.2014.12.046

38. Wen, L., Gao, Q., Ma, C.W., Ge, Y., You, L., Liu, R.H., Fu, X., Liu, D. (2016). Effect of polysaccharides from *Tremella fuciformis* on UV-induced photoaging. *Journal of Functional Foods*, *20*, 400–410.
https://doi.org/10.1016/j.jff.2015.11.014

39. Wu, J., Li, P., Tao, D., Zhao, H., Sun, R., Ma, F., Zhang, B. (2018). Effect of solution plasma process with hydrogen peroxide on the degradation and antioxidant activity of polysaccharide from *Auricularia auricula*. *International Journal of Biological Macromolecules*, *117*, 1299–1304.
https://doi.org/10.1016/j.ijbiomac.2018.05.191

40. Wu, Y.J., Wei, Z.X., Zhang, F.M., Linhardt, R.J., Sun, P.L., Zhang, A.Q. (2019). Structure, bioactivities and applications of the polysaccharides from *Tremella fuciformis* mushroom: A review. *International Journal of Biological Macromolecules*, *121*, 1005–1010.
https://doi.org/10.1016/j.ijbiomac.2018.10.117

41. Xiao, H., Li, H., Wen, Y., Jiang, D., Zhu, S., He, X., Xiong, Q., Gao, J., Hou, S., Huang, S., He, L., Liang, J. (2021). *Tremella fuciformis* polysaccharides ameliorated ulcerative colitis *via* inhibiting inflammation and enhancing intestinal epithelial barrier function. *International Journal of Biological Macromolecules*, *180*, 633–642.
https://doi.org/10.1016/j.ijbiomac.2021.03.083

42. Xu, Y., Xie, L., Zhang, Z., Zhang, W., Tang, J., He, X., Zhou, J., Peng, W. (2021). *Tremella fuciformis* polysaccharides inhibited colonic inflammation in dextran sulfate sodium-treated mice *via* Foxp3+ T cells, gut microbiota, and bacterial metabolites. *Frontiers in Immunology*, *12*, art. no. 648162.
https://doi.org/10.3389/fimmu.2021.648162

43. Xu, Y., Zhang, X., Yan, X.H., Zhang, J.L., Wang, L.Y., Xue, H., Jiang, G.C., Ma, X.T., Liu, X.J. (2019). Characterization, hypolipidemic and antioxidant activities of degraded polysaccharides from *Ganoderma lucidum*. *International Journal of Biological Macromolecules*, *135*, 706–716.
https://doi.org/10.1016/j.ijbiomac.2019.05.166

44. Yang, D., Liu, Y., Zhang, L. (2019). Chapter Sixteen - *Tremella* polysaccharide: The molecular mechanisms of its drug action. In L. Zhang (Ed.) *Progress in Molecular Biology and Translational Science*, Academic Press, pp. 383–421.
https://doi.org/10.1016/bs.pmbts.2019.03.002

45. Ye, S., Liu, F., Wang, J., Wang, H., Zhang, M. (2012). Antioxidant activities of an exopolysaccharide isolated and purified from marine *Pseudomonas* PF-6. *Carbohydrate Polymers*, *87*(1), 764–770.
https://doi.org/10.1016/j.carbpol.2011.08.057

46. Zhang, J., Zhao, X., Jiang, Y., Zhao, W., Guo, T., Cao, Y., Teng, J., Hao, X., Zhao, J., Yang, Z. (2017). Antioxidant status and gut microbiota change in an aging mouse model as influenced by exopolysaccharide produced by *Lactobacillus plantarum* YW11 isolated from Tibetan kefir. *Journal of Dairy Science*, *100*(8), 6025–6041.
https://doi.org/10.3168/jds.2016-12480

47. Zhang, L., Li, X., Xu, X., Zeng, F. (2005). Correlation between antitumor activity, molecular weight, and conformation of lentinan. *Carbohydrate Research*, *340*(8), 1515–1521.
https://doi.org/10.1016/j.carres.2005.02.032

48. Zhang, L., Ye, X., Ding, T., Sun, X., Xu, Y., Liu, D. (2013). Ultrasound effects on the degradation kinetics, structure and rheological properties of apple pectin. *Ultrasonics Sonochemistry*, *20*(1), 222–231.
https://doi.org/10.1016/j.ultsonch.2012.07.021

49. Zhang, Z., He, S., Cao, X., Ye, Y., Yang, L., Wang, J., Liu, H., Sun, H. (2020). Potential prebiotic activities of soybean peptides Maillard reaction products on modulating gut microbiota to alleviate aging-related disorders in D--galactose-induced ICR mice. *Journal of Functional Foods*, *65*, art. no. 103729.
https://doi.org/10.1016/j.jff.2019.103729

50. Zhang, Z., Sun, D., Xu, M., Tian, H., Pan, J. (2014). Study on the antioxidation effect of *Tremella* polysaccharide. *Food Research and Development*, *18*, 10–15.

51. Zhao, L., Zhang, F., Ding, X., Wu, G., Lam, Y.Y., Wang, X., Fu, H., Xue, X., Lu, C., Ma, J., Yu, L., Xu, C., Ren, Z., Xu, Y., Xu, S., Shen, H., Zhu, X., Shi, Y., Shen, Q., Dong, W., Liu, R., Ling, Y., Zeng, Y., Wang, X., Zhang, Q., Wang, J., Wang, L., Wu, Y., Zeng, B., Wei, H., Zhang, M., Peng, Y., Zhang, C. (2018). Gut bacteria selectively promoted by dietary fibers alleviate type 2 diabetes. *Science*, *359*(6380), 1151–1156.
https://doi.org/10.1126/science.aao5774

52. Zhao, X., Yi, R., Zhou, X., Mu, J., Long, X., Pan, Y., Song, J.L., Park, K.Y. (2019). Preventive effect of *Lactobacillus plantarum* KSFY02 isolated from naturally fermented yogurt from Xinjiang, China, on D-galactose–induced oxidative aging in mice. *Journal of Dairy Science*, *102*(7), 5899–5912.
https://doi.org/10.3168/jds.2018-16033